Assessment of peri-implant defects at titanium and zirconium dioxide implants by means of periapical radiographs and cone beam computed tomography: An in-vitro examination

Steiger-Ronay, Valerie ; Krcmaric, Zvonimir ; Schmidlin, Patrick R ; Sahrmann, Philipp ; Wiedemeier, Daniel B ; Benic, Goran I

Abstract: OBJECTIVE To test the accuracy of measurement of interproximal peri-implant bone defects at titanium (Ti) and zirconium dioxide (ZrO) implants by digital periapical radiography (PR) and cone beam computed tomography (CBCT). MATERIAL AND METHODS A total of 18 models, each containing one Ti and one ZrO implant, were cast in dental stone. Six models each were allocated to following defect groups: A-no peri-implant defect, B-1 mm width defect, C-1.5 mm width defect. The defect width was measured with a digital sliding caliper. Subsequently, the models were scanned by means of PR and CBCT. Three examiners assessed the defect width on PR and CBCT. Wilcoxon signed-rank test and Wilcoxon rank sum test were applied to detect differences between imaging techniques and implant types. RESULTS For PR, the deviation of the defect width measurement (mm) for groups A, B, and C amounted to 0.01 ± 0.03, -0.02 ± 0.06, and -0.00 ± 0.04 at Ti and 0.05 ± 0.02, 0.01 ± 0.03, and 0.09 ± 0.03 at ZrO implants. The corresponding values (mm) for CBCT reached 0.10 ± 0.11, 0.26 ± 0.05, and 0.24 ± 0.08 at Ti and 1.07 ± 0.06, 0.64 ± 0.37, and 0.54 ± 0.17 at ZrO implants. Except for Ti with defect A, measurements in PR were significantly more accurate in comparison to CBCT (p 0.05). Both methods generally yielded more accurate measurements for Ti than for ZrO . CONCLUSIONS The assessment of interproximal peri-implant defect width at Ti and ZrO implants was more accurate in PR in comparison to CBCT. Measurements in CBCT always led to an overestimation of the defect width, reaching clinical relevance for ZrO implants.

DOI: https://doi.org/10.1111/clr.13383

Assessment of peri-implant defects at titanium and zirconium dioxide implants by means of periapical radiographs and cone beam computed tomography: an in-vitro examination

Valerie Steiger-Ronay*, Zvonimir Krcmaric**, Patrick R. Schmidlin*, Philipp Sahrmann*, Daniel B. Wiedemeier***, Goran I. Benic****

* Clinic of Preventive Dentistry, Periodontology and Cariology, Center of Dental Medicine, University of Zurich, Zurich, Switzerland

** Private Practice, Zurich, Switzerland

*** Statistical Services, Center of Dental Medicine, University of Zurich, Switzerland

**** Clinic of Fixed and Removable Prosthodontics and Dental Material Science, Center of Dental Medicine, University of Zurich, Zurich, Switzerland

Running title: Radiographic assessment of peri-implant defects

Keywords: Peri-implantitis, bone, bone defect, computed tomography, cone beam computed tomography, CBCT, periapical radiography, X-ray, dental implant, zirconium dioxide, titanium, zirconium dioxide implant, titanium implant, digital, radiology, scan

Correspondence:
Patrick R. Schmidlin
Clinic of Preventive Dentistry, Periodontology and Cariology
Plattenstrasse 11, 8032 Zürich, Switzerland
Phone +41 44 634 32 84
Fax: +41 44 634 43 08
E-mail patrick.schmidlin@zzm.uzh.ch

Abstract

Objective: To test the accuracy of measurement of interproximal peri-implant bone defects at titanium (Ti) and zirconium dioxide (ZrO_2) implants by digital periapical radiography (PR) and cone beam computed tomography (CBCT).

Material and Methods: A total of 18 models, each containing one Ti and one ZrO_2 implant, were cast in dental stone. Six models each were allocated to following defect groups: A - no peri-implant defect, B - 1 mm width defect, C - 1.5 mm width defect. The defect width was measured with a digital sliding caliper. Subsequently, the models were scanned by means of PR and CBCT. Three examiners assessed the defect width on PR and CBCT. Wilcoxon signed-rank test and Wilcoxon rank sum test were applied to detect differences between imaging techniques and implant types.

Results: For PR the deviation of the defect width measurement (mm) for groups A, B and C amounted to 0.01±0.03, -0.02±0.06 and -0.00±0.04 at Ti and 0.05±0.02, 0.01±0.03 and 0.09±0.03 at ZrO_2 implants. The corresponding values (mm) for CBCT reached 0.10±0.11, 0.26± 0.05 and 0.24±0.08 at Ti and 1.07±0.06, 0.64±0.37 and 0.54±0.17 at ZrO_2 implants. Except for Ti with defect A, measurements in PR were significantly more accurate in comparison to CBCT ($p \leq 0.05$). Both methods generally yielded more accurate measurements for Ti than for ZrO2.

Conclusions: The assessment of interproximal peri-implant defect width at Ti and ZrO_2 implants was more accurate in PR in comparison to CBCT. Measurements in CBCT always led to an overestimation of the defect width, reaching clinical relevance for ZrO_2 implants.

Introduction

Peri-implantitis prevalence at 5-10 years was reported to range from 20 to 28% on subject level and from 10 to 12% on implant level, depending on the criteria applied for the analysis and the population under investigation (Mombelli et al. 2012; Atieh et al. 2013). In practice, when characteristic clinical signs such as increased probing pocket depth, concomitant bleeding or suppuration on probing indicate the presence of peri-implant disease, a radiographic evaluation of the peri-implant bone level is recommended (Lindhe and Meyle 2008). The conventional intra-oral periapical radiography (PR) is the most commonly used technique for the assessment of peri-implant bone. This imaging technique, however, is limited to two planes. Therefore, unfavorable marginal bone levels or the absence of osseointegration may be hidden by superimposition (Isidor 1997).

Cone beam computed tomography (CBCT) has the potential to overcome some of the limitations encountered with PR. It allows for the 3D examination of dental implants and their surrounding tissues. Due to this advantage, CBCT became a widely used technique for the examination of facial and oral bone conditions at dental implants in clinical research (Benic et al. 2012;Jung et al. 2013). Drawbacks like the higher radiation dose and the increased costs in comparison to intraoral techniques, however, need to be mentioned in this context (Harris et al. 2012). Another shortcoming of CBCT is its susceptibility to artifacts (Schulze et al. 2010; Schulze et al. 2011; Esmaeili et al. 2013). Particularly radio-opaque objects such as crowns and implants cause artifacts in CBCT and, therefore, hamper the diagnosis of potential bone defects in the adjacent areas. Schulze and colleagues analyzed CBCT artifacts induced by titanium implants embedded in dental stone. Artifacts were observed predominantly in the interproximal regions between the implants, rendering the evaluation of these areas very difficult (Schulze et al. 2010). Blooming artifacts around implants may obscure most of the peri-implant area (Codari et al. 2017; Jacobs et al. 2018). Therefore, the question can be raised whether CBCT imaging represents an adequate technique for the detailed assessment of structures in the close proximity of dental implants.

The aim of this study was to test the accuracy of measurements of interproximal peri-implant defects at titanium (Ti) and zirconium dioxide (ZrO_2) implants by periapical radiography (PR) and cone beam computed tomography (CBCT).

Materials & Methods

Bone block models

A total of 18 models were prepared as follows: 100 g of white articulation cement (Artifix Artikulationsgips, Amann Girrbach AG, Pforzheim, Germany) and 20 g of sawdust, which has been previously colored with red ink (Pelikan AG, Hannover, Germany), were mixed with 30 ml of distilled water. After hardening, standardized models were ground under constant water-cooling into uniform blocks measuring 45 x 14 x 12 mm. Each of these models was allocated to receive one titanium implant **(**Straumann SLActive 4.1 mm x 8 mm, Institut Straumann AG, Basel, Switzerland) and one zirconium dioxide implant (ceramic.implant by vitaclinical, 3.5 mm x 4.5 mm x 10 mm, VITA Zahnfabrik, Bad Säckingen, Germany) in a set distance of 25 mm. A precision drill and a parallelometer were used to prepare the two implant beds for receiving the Ti and the ZrO_2 implants according to the manufacturers' instructions. Thereafter, the implant beds were expanded, as applicable, to represent one of the following three defect configurations (6 models each):

1) Defect configuration A: No peri-implant defect (0 mm) was created for either implant type
2) Defect configuration B: A peri-implant defect of 1 mm for the Ti implant and 0.9 mm for the ZrO_2 implant was created.
3) Defect configuration C: A peri-implant defect of 1.5 mm for the Ti implant and 1.4 mm the ZrO_2 implant was created.

Determination of effective defect dimensions by caliper

Before insertion of the implants, the effective internal diameter of each defect was measured with a digital sliding caliper (American Dental Systems, Vaterstetten, Germany). The exact dimension was always determined at the widest circumference of the cervical third of the defect. Lastly, the two different implants were inserted in the center of their defect beds and were fixed herein with the help of dental wax (Dentsply, Ballaigues, Switzerland).

Image acquisition

Each model was scanned once by means of conventional PR (Trophy Iris CCX, Trophy Radiologie, Kehl, Germany) and once by means of CBCT (KaVo 3D eXam, KaVo Dental AG, Biberach, Germany). For the scanning procedure, the study models were positioned on the according supporting plate provided by the manufacturer, always placed in the center of the field-of-view (FOV). Following parameters were applied for the image acquisition by conventional periapical radiography: 65kV, 8mA beam current, and a scanning time of 0.10 s. The CBCT scans were obtained with following parameters: 120 kV, 5 mA beam current, FOV

diameter of 16 cm, FOV height of 6 cm, 600 projections, 360° rotation, voxel size of 0.25 mm, slice thickness of 1mm, window width/window level of 1250/250 and a scanning time of 26 s.

Determination of defect dimensions on PR and CBCT scans

For the analysis of the PR scans, the defect measurement was performed using ImageJ software (NIH, USA, http:// rsb.info.nih.gov/ij/), while the CBCT scans were analyzed by Osirix software (Osirix Imaging Software, Pixmeo SARL, Bernex, Siwtzerland). Three blinded examiners performed all measurements twice with an interval of three weeks. The two measurements were averaged thereafter. Lateral reconstructions perpendicular to the implant's longitudinal axis were used for the CBCT data evaluation. Defect measurements were always performed in *mesio-distal* direction at the largest defect circumference in the cervical third of the implant. They were carried out on both sides of the implant body to the respective defect wall, perpendicular to the implant's longitudinal axis (Figure 1). These measurements of both sides of the implant were then added up and divided in half to compensate for any unintended implant tilting within the prepared implant bed.

Determination of difference between effective and measured defect dimensions

For determining the difference between the effective (as determined by caliper) and the measured defect dimensions (as determined on PR/CBCT scans), i.e. the measurement accuracy, the radiographic defect measure was subtracted from the value determined by digital sliding caliper. Therefore positive values indicate an overestimation, and negative values an underestimation of the true defect.

Statistical analyses

For assessing the examiners' inter-rater reliability, the intraclass correlation (two-way, consistency) was calculated. Thereafter, the data was averaged over the 3 examiners to yield a mean difference between effective and measured defect, i.e. a mean measurement error per image taken. Descriptive statistics such as mean, standard deviation, median and IQR were computed. The Wilcoxon signed-rank test was applied to evaluate differences between the two imaging techniques, splitted by defect type and implant material. Differences between the two implant materials were analyzed by the Wilcoxon rank sum test. Results of statistical analyzes with p-values smaller than 0.05 were considered to be statistically significant. All statistical analyses and plots were done with the statistical software R (Team 2015), including the irr and ggplot2 packages (Gamer et al. 2012; Wickham 2009).

Results

Inter-examiner reproducibility was very good (Fleiss 1981), with an estimated intraclass-correlation of 0.78. Intra-examiner reproducibility was also excellent in two of the three examiners and moderate in the third one with intraclass-correlations of 0.98, 0.99 and 0.54, respectively.

For PR the average deviation of the defect width measurements for groups A, B and C amounted to 0.01 ± 0.03 mm, -0.02 ± 0.06 mm and -0.00 ± 0.04 mm at Ti implants and 0.05 ± 0.02 mm, 0.01 ± 0.03 mm and 0.09 ± 0.03 mm at ZrO_2 implants. The corresponding values for CBCT amounted to 0.10 ± 0.11 mm, 0.26 ± 0.05 mm and 0.24 ± 0.08 mm at Ti implants and 1.07 ± 0.06 mm, 0.64 ± 0.37 mm and 0.54 ± 0.17 mm at ZrO_2 implants (Table 1, Figure 2). Measurements on the CBCT scans always led to an overestimation of the defect.

Measurements in PR were always significantly more accurate in comparison to CBCT ($p \leq 0.05$) except for Ti and defect type A, where no significant difference between the two imaging techniques could be found (Table 2). For Ti implants the mean difference in the measurement error between PR und CBCT ranged from -0.09 mm to -0.28 mm. For ZrO_2 implants, the corresponding parameter ranged from -0.45 mm to -1.02 mm.

Measurements at Ti implants were generally more accurate in comparison to ZrO_2 implants ($p \leq 0.05$) for both methods, except for PR and defect B, where the measurement error between the two materials was not significantly different (Table 3). For PR the mean difference in the measurement error between Ti und ZrO_2 ranged from -0.03 mm to -0.09 mm. For CBCT, the inaccuracy at ZrO_2 was considerably higher as compared to Ti implants (Table 3). Thus, for CBCT, the mean difference in the measurement error between Ti und ZrO_2 ranged from -0.30 mm to -0.97 mm (Table 3).

Discussion

Diagnostic radiographic imaging is essential for the detection, treatment planning and monitoring of peri-implant diseases. The present study assessed the accuracy of interproximal peri-implant defect measurements performed in PR and CBCT. The difference between the measurement methods was assessed with two different implant materials (Ti and ZrO_2) and different defect dimensions were evaluated.

It has been shown that in the interpretation of CBCT images, artifacts adjacent to Ti implants are a common finding that may hinder the correct interpretation of the peri-implant situation

(Schulze et al. 2010). The presence of these CBCT artifacts around Ti implants are independent of implant position and present with a geometrical pattern (Benic et al. 2013): increased gray values are found at the buccal and the lingual aspects, whereas regions with reduced gray values are located along the long axis of the mandibular body. Concomitant with these findings, the present in-vitro study also proved more artifacts to be present on CBCT as compared to PR scans, resulting in an according impairment of measurement quality. With regard to measurement errors, the examination of the PR scans always provided superior results. This finding was especially true for the ZrO_2, but to a lesser extent also for Ti implants.

Two implant systems made from different materials, i.e. titanium and zirconium dioxide were tested in this study. Titanium has been established as the preferred metal for dental implants owing to its unique mechanical properties as well as its high resistance to corrosion (Depprich et al. 2014). Lately zirconium dioxide got more popular as a biocompatible and aesthetical alternative because of its biophysical properties and white color. In addition to the mentioned characteristics, implant composition has a significant influence on radiographic image quality and artifact intensity. A recent publication which analyzed CBCT scans showed that ZrO_2 implants generate significantly more artifacts as compared to Ti or titanium-zirconium implants, which furthermore presented with an up to three-fold intensity (Sancho-Puchades et al. 2015). The results of the present investigation confirm these patterns. Measurements on ZrO_2 implants almost always presented with more inaccuracies than Ti implants. This finding was more pronounced on CBCT scans, where - irrespective of defect type - a clinically significant overestimation of defect dimensions of up to 1.1 mm was found.

The fact that this *in vitro* set-up was based on the use of dental plaster models may be considered as a limitation of the present investigation. No attenuation material to mimic the soft tissues surrounding the dental implants was used. Further, block radiography is not the ideal precondition for CBCT analysis due to the lack of surrounding tissues as presumed by the reconstruction algorithm, which will lead to altered image quality, defect contrast and artifact development. The clinical situation of conventional PR or CBCT scanning could therefore only be partially simulated. Nevertheless, previous studies which were looking at the accuracy of CBCT imaging also used some modification of block radiography such as bovine bone rips (Razavi et al. 2010) or mandibular plaster models (Schulze et al. 2010). Reproducible settings as well as the homogenous structure of the dental plaster models allowed for repeated analyses by different examiners under similar conditions.

Another limitation of the present study was the difference of analyzed defect widths. These were not identical for Ti and ZrO_2 implants for defect configurations B (1 mm for the Ti and 0.9 mm for the ZrO_2 implant) and C (defect of 1.5 mm for the Ti and 1.4 mm the ZrO_2 implant). This fact was due to the investigation of implants of different design and diameter, which were inserted into predetermined defects as produced by a precision drill. This lack of complete standardization, and the inclusion of solely linear measurements by a digital sliding caliper left some space for variability. For the determination of the radiographic defect measurement accuracy, however, absolute values in mm were determined for both implant types, therefore providing comparable results.

Ti and ZrO_2 implants were tested side-by-side as they were embedded in the same plaster model. This set-up has some advantages, such as having both implant types scanned in the same recording. Whenever a scan is repeated, minimal variance is possible, a problem that was avoided through this set-up. One possible disadvantage could have been a superimposition of artifacts projected around the Ti and ZrO_2 implants influencing each other. It was shown, however, that a significant decrease in artifact intensity is found with increasing distance from the implant surface (Benic et al. 2013). Therefore this effect would have been minimal if at all recognizable.

Circumferential peri-implant defects are the most common finding in advanced peri-implant lesions. In this context, one of the main advantages of CBCT imaging is the ability to also depict the vestibular and lingual implant situation, which PR cannot show. Hence, it would have been of interest to investigate the lingual and buccal aspects of the Ti and ZrO_2 implants as well. Furthermore, CBCT data could have been compared and analyzed three-dimensionally and not just by linear measurements. This study, however, focused on the comparison between the 2D and 3D techniques, which rendered this aspect impossible to compare. Nevertheless, it has been shown that intra-operatively assessed peri-implant bone levels are similar at all circumferential positions around an implant (García-García et al. 2016). Furthermore, artefacts around implants in CBCT images are distributed according to a geometrical pattern with a similar circumferential presentation (Benic et al. 2013). Therefore, if no interproximal peri-implant defects are recognizable on CBCT images, it can be assumed that the bone levels are similar on the buccal and lingual implant aspects. Considering the fact that PR still presents the gold standard in the diagnostic of interproximal peri-implant defects, which also requires less radiation than CBCT imaging, one can derive the high importance of right indication setting.

In this investigation inter- and intra-examiner reproducibility was found to be very good with a small range of differences amounting to approximately 0.07 mm for inter-examiner and 0.05 mm for intra-examiner data. Both were thus below the CBCT resolution of 0.25 mm and could therefore be assumed to be random. This finding suggests that the actual resolution for users may be better than the proclaimed 0.25 mm.

The described results may not be generalized, as CBCT scanners by different manufacturers with different spatial resolutions (voxel sizes), fields of view (FOV), patient positioning systems or duration of scan exist, which will influence the quality and interpretability of the scans (Razavi et al. 2010). Therefore, guidelines for the use of diagnostic imaging in implant dentistry were published by the European Association for Osseointegration (EAO) with the aim of obtaining diagnostic information with as low as reasonably achievable (ALARA principle) radiation exposure (Harris et al. 2012). In this publication technical recommendations were given for PR (mSv: 0.002-0.006/radiograph; use of F-speed film, rectangular collimation and paralleling technique) as well as CBCT imaging (mSv: <0.5/jaw; KV: 120; mAs: < 100; Slice thickness: 1 mm; Pitch: 1–1.5; suggested window: 1250 / window level: 250). The detectability of peri-implant bone defects can be further optimized by adjustment and customization of image pre-settings ("filters") in CBCT imaging software, as shown in a recent study (de-Azevedo-Vaz et al. 2013). Radiation dose reduction is possible by decreasing the number of slices, increasing pitch and lowering mAs (Harris et al. 2012). Future studies should focus on these important aspects, as radiation exposure to patients should always be kept as low as reasonably achievable. The benefits of radiographic investigations must at all times outweigh any potential risks to the patient.

Conclusions

Within the limitations of the present in-vitro investigation it can be concluded that:

- The assessment of interproximal peri-implant defect width at Ti and ZrO_2 implants is more accurate in periapical radiography in comparison to CBCT.
- Measurements in CBCT result in an overestimation of the defect size.
- Inaccuracies in the assessments of interproximal peri-implant defects on CBCT are more pronounced at ZrO2 implants as compared to Ti implants.

Acknowledgements

The implants were kindly provided by Straumann AG, Basel, Switzerland and VITA Zahnfabrik, Bad Säckingen, Germany.

Figures

Figure 1

Representative images for periapical radiography (A) and CBCT (B). Measurements of the defect width were performed on both sides of the implants as indicated by the arrows.

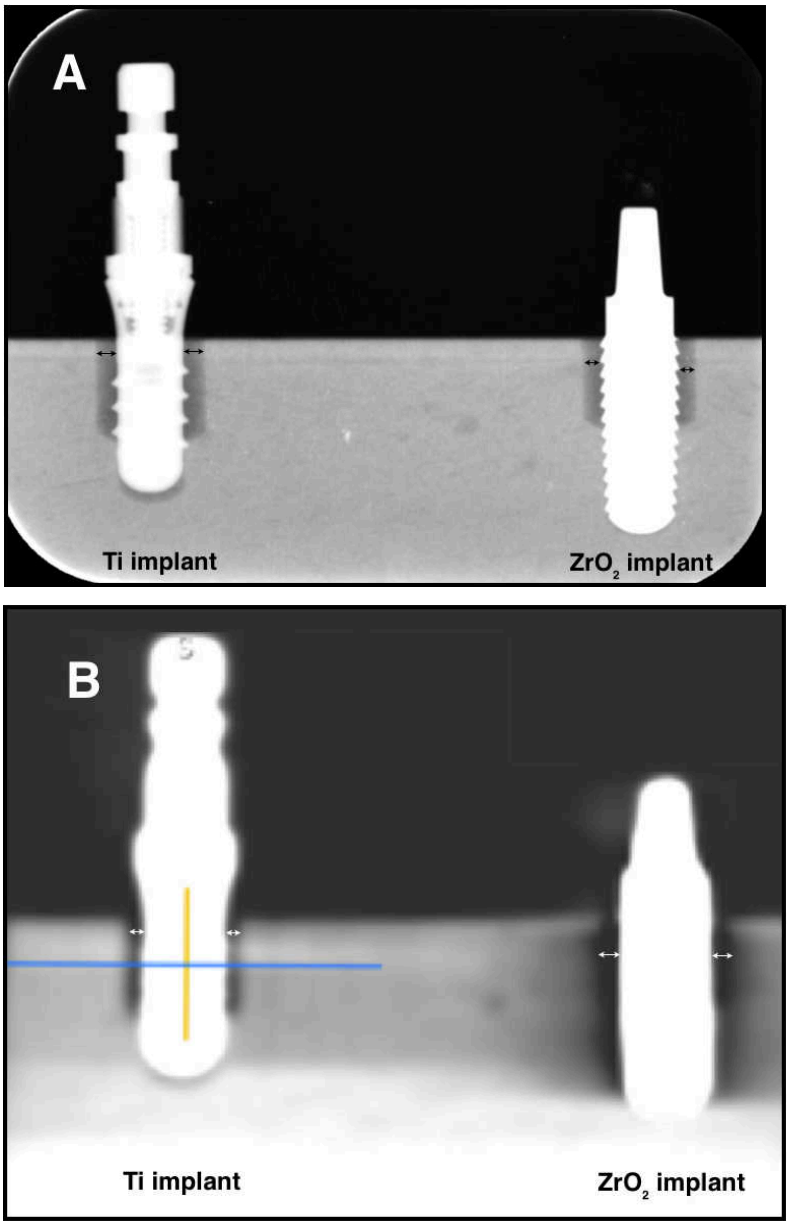

Figure 2

Box-plot representing the measurement error (in mm) for different imaging techniques, implant types and defect widths. Positive values represent an overestimation of the defect size.

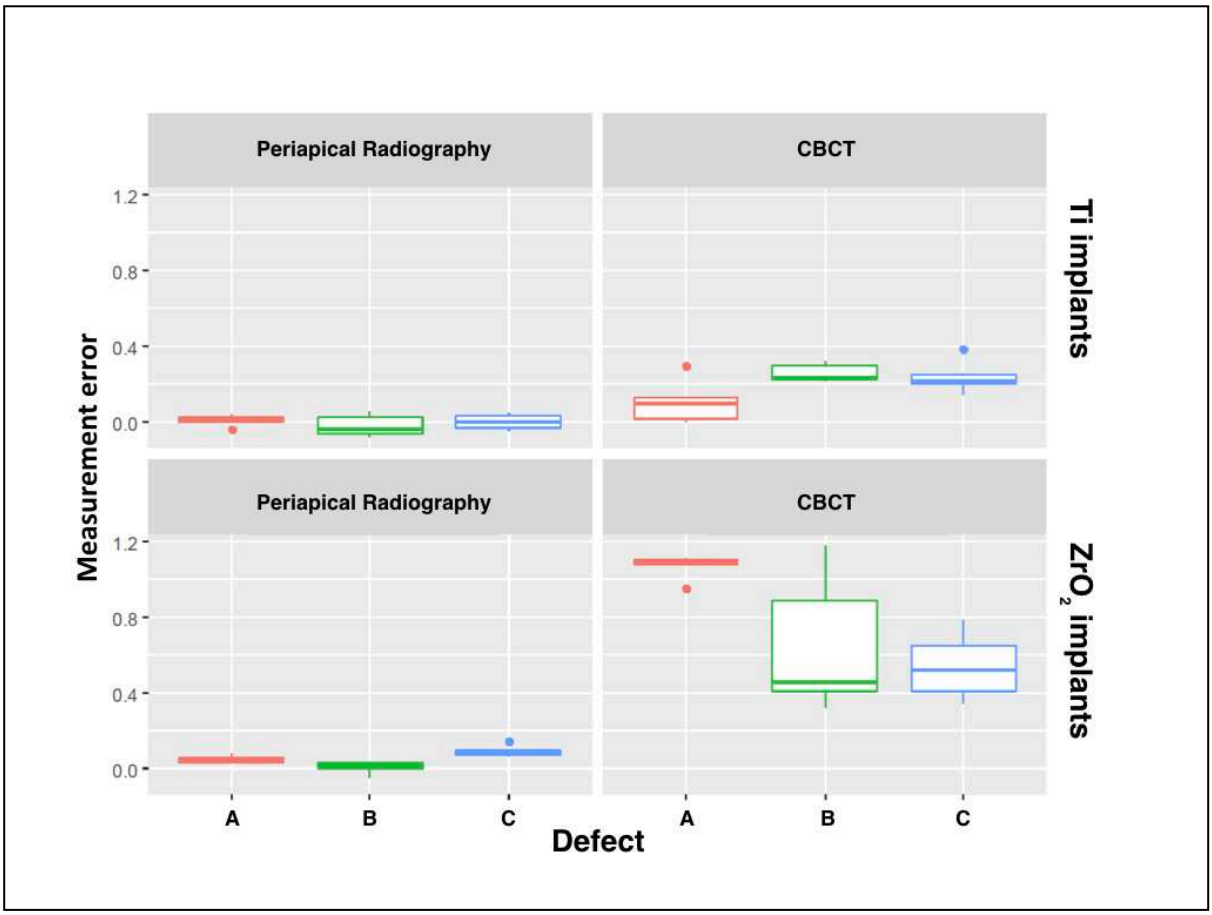

Tables

Table 1

Results of the measurement error (in mm) for different imaging techniques, implant types and defect widths. Positive values represent an overestimation of the defect width.

	Implant Material	Defect Type								
		Defect A			Defect B			Defect C		
		Mean ± SD	Median	IQR	Mean ± SD	Median	IQR	Mean ± SD	Median	IQR
PR	Ti	0.01 ± 0.03	0.02	0.03	-0.02 ± 0.06	-0.04	0.09	-0.00 ± 0.04	-0.00	0.06
	ZrO_2	0.05 ± 0.02	0.05	0.02	0.01 ± 0.03	0.02	0.03	0.09 ± 0.03	0.09	0.02
CBCT	Ti	0.10 ± 0.11	0.10	0.11	0.26 ± 0.05	0.23	0.08	0.24 ± 0.08	0.22	0.05
	ZrO_2	1.07 ± 0.06	1.09	0.02	0.64 ± 0.37	0.46	0.48	0.54 ± 0.17	0.52	0.24

PR, periapical radiography; CBCT, cone beam computed tomography; Ti, titanium implant; ZrO_2, zirconium dioxide implant; SD, standard deviation; IQR, interquartile range

Table 2

Differences of the measurement error (in mm) between periapical radiographs and CBCT.

Defect Type	Ti		ZrO_2	
	Mean ± SD	**p-value***	**Mean ± SD**	**p-value***
A	-0.09 ± 0.12	0.16	-1.02 ± 0.06	0.04†
B	-0.28 ± 0.07	0.03†	-0.63 ± 0.35	0.04†
C	-0.24 ± 0.09	0.03†	-0.45 ± 0.19	0.03†

Ti, titanium implant; ZrO_2, zirconium dioxide implant; SD, standard deviation
* Results of Wilcoxon signed-rank test.
† Statistically significant.

Table 3

Differences of the measurement error (in mm) between titanium and zirconium dioxide implants.

Defect Type	PR		CBCT	
	Mean ± SD	***p*-value***	**Mean ± SD**	***p*-value***
A	-0.04 ± 0.02	0.02†	-0.97 ± 0.12	0.00†
B	-0.03 ± 0.06	0.052	-0.38 ± 0.34	0.00†
C	-0.09 ± 0.04	0.00†	-0.30 ± 0.11	0.01†

PR, periapical radiography; CBCT, cone beam computed tomography; SD, standard deviation
* Results of Wilcoxon rank-sum test.
† Statistically significant.

References

Atieh, M.A., Alsabeeha, N.H., Faggion, C.M.J. & Duncan, W.J. (2013) The frequency of peri-implant diseases: a systematic review and meta-analysis. *J Periodontol* **84**: 1586-98. 10.1902/jop.2012.120592.

Benic, G.I., Mokti, M., Chen, C.J., Weber, H.P., Hammerle, C.H. & Gallucci, G.O. (2012) Dimensions of buccal bone and mucosa at immediately placed implants after 7 years: a clinical and cone beam computed tomography study. *Clin Oral Implants Res* **23**: 560-6. 10.1111/j.1600-0501.2011.02253.x.

Benic, G.I., Sancho-Puchades, M., Jung, R.E., Deyhle, H. & Hammerle, C.H. (2013) In vitro assessment of artifacts induced by titanium dental implants in cone beam computed tomography. *Clin Oral Implants Res* **24**: 378-83. 10.1111/clr.12048

Codari, M., de Faria Vasconcelos, K., Ferreira Pinheiro Nicolielo, L., Haiter Neto, F. & Jacobs, R. (2017) Quantitative evaluation of metal artifacts using different CBCT devices, high-density materials and field of views. *Clin Oral Implants Res* **28**: 1509-14. 10.1111/clr.13019.

de-Azevedo-Vaz, S.L., Alencar, P.N., Rovaris, K., Campos, P.S. & Haiter-Neto, F. (2013) Enhancement cone beam computed tomography filters improve in vitro periimplant dehiscence detection. *Oral Surg Oral Med Oral Pathol Oral Radiol* **116**: 633-9. 10.1016/j.oooo.2013.06.029.

Depprich, R., Naujoks, C., Ommerborn, M., Schwarz, F., Kubler, N.R. & Handschel, J. (2014) Current findings regarding zirconia implants. *Clin Implant Dent Relat Res* **16**: 124-37. 10.1111/j.1708-8208.2012.00454.x.

Esmaeili, F., Johari, M. & Haddadi, P. (2013) Beam hardening artifacts by dental implants: Comparison of cone-beam and 64-slice computed tomography scanners. *Dent Res J (Isfahan)* **10**: 376-81.

Fleiss, J.L. (1981) Statistical Methods for Rates and Proportions. (2nd ed.). Hoboken, NJ.: Wiley.

Gamer, M., Lemon, J. & Fellows Puspendra Singh, I. (2012) Irr: Various Coefficients of Interrater Reliability and Agreement. R package version 0.84.

García-García, M., Mir-Mari, J., Benic, G.I., Figueiredo, R. & Valmaseda-Castellón, E. (2016) Accuracy of periapical radiography in assessing bone level in implants affected by peri-implantitis: a cross-sectional study. *J Clin Periodontol* **43**: 85-91. 10.1111/jcpe.12491.

Harris, D., Horner, K., Grondahl, K., Jacobs, R., Helmrot, E., Benic, G.I., Bornstein, M.M., Dawood, A. & Quirynen, M. (2012) E.A.O. guidelines for the use of diagnostic imaging in implant dentistry 2011. A consensus workshop organized by the European Association for Osseointegration at the Medical University of Warsaw. *Clin Oral Implants Res* **23**: 1243-53. 10.1111/j.1600-0501.2012.02441.x.

Isidor, F. (1997) Clinical probing and radiographic assessment in relation to the histologic bone level at oral implants in monkeys. *Clin Oral Implants Res* **8**: 255-64.

Jacobs, R., Salmon, B., Codari, M., Hassan, B. & Bornstein, M.M. (2018) Cone beam computed tomography in implant dentistry: recommendations for clinical use. *BMC Oral Health* **18**: 88. 10.1186/s12903-018-0523-5.

Jung, R.E., Philipp, A., Annen, B.M., Signorelli, L., Thoma, D.S., Hammerle, C.H., Attin, T. & Schmidlin, P. (2013) Radiographic evaluation of different techniques for ridge preservation after tooth extraction: a randomized controlled clinical trial. *J Clin Periodontol* **40**: 90-8. 10.1111/jcpe.12027.

Lindhe, J. & Meyle, J. (2008) Peri-implant diseases: Consensus Report of the Sixth European Workshop on Periodontology. *J Clin Periodontol* **35**: 282-5. 10.1111/j.1600-051X.2008.01283.x.

Mombelli, A., Muller, N. & Cionca, N. (2012) The epidemiology of peri-implantitis. *Clin Oral Implants Res* **23** Suppl 6: 67-76. 10.1111/j.1600-0501.2012.02541.x

R Core Team. (2015) R: A language and environment for statistical computing. Vienna, Austria: R Foundation for Statistical Computing. URL https://www.R-project.org/.

Razavi, T., Palmer, R.M., Davies, J., Wilson, R. & Palmer, P.J. (2010) Accuracy of measuring the cortical bone thickness adjacent to dental implants using cone beam computed tomography. *Clin Oral Implants Res* **21**: 718-25. 10.1111/j.1600-0501.2009.01905.x.

Sancho-Puchades, M., Hämmerle, C.H. & Benic, G.I. (2015) In vitro assessment of artifacts induced by titanium, titanium-zirconium and zirconium dioxide implants in cone-beam computed tomography. *Clin Oral Implants Res* **26**: 1222-8. 10.1111/clr.12438

Schulze, R., Heil, U., Gross, D., Bruellmann, D.D., Dranischnikow, E., Schwanecke, U. & Schoemer, E. (2011) Artefacts in CBCT: a review. *Dentomaxillofac Radiol* **40**: 265-73. 10.1259/dmfr/30642039.

Schulze, R.K., Berndt, D. & d'Hoedt, B. (2010) On cone-beam computed tomography artifacts induced by titanium implants. *Clin Oral Implants Res* **21**: 100-7. 10.1111/j.1600-0501.2009.01817.x.

Wickham, H. (2009) Ggplot2: Elegant Graphics for Data Analysis. New York: Springer-Verlag.